High-Precision Photogrammetric 3D Modeling Technology Based on Multi-Source Data Fusion and Deep Learning-Enhanced Feature Learning Using Internet of Things Big Data

Guangtao Zhang[1], Jun Zhang[2, 3*]
[1]College of Information Engineering, Yangzhou Polytechnic College, Yangzhou 225000, Jiangsu, China
[2]Center of Engineering Training, Yangzhou Polytechnic College, Yangzhou 225000, Jiangsu, China
[3]Jiangsu Safety & Environment Technology and Equipment for Planting and Breeding Industry Engineering Research Center, Yangzhou 225000, Jiangsu, China
E-mail: zhang-jun168@hotmail.com
*Corresponding author

Keywords: internet of things, big data, high-precision photography, 3D modeling technology

Received: August 15, 2024

As technology advances and application demands grow, high-precision three-dimensional (3D) modeling is increasingly essential for urban planning, disaster management, and cultural heritage protection. This study presents a high-precision photogrammetric 3D modeling approach with a focus on integrating multi-source data fusion techniques for complex terrains. The methodology incorporates aerial imagery, LiDAR data, ground survey data, and meteorological corrections, covering the entire workflow from data preprocessing, feature extraction, and registration to multi-source data fusion. Key innovations include an adaptive weight adjustment strategy, global optimization registration techniques, and deep learning-assisted feature learning, all contributing to significant improvements in model accuracy and reliability. Experimental results show a X% improvement in spatial accuracy and a Y% reduction in mean squared error (MSE), along with enhanced morphological structure recovery and visual effects. These improvements have been validated through practical applications and received positive feedback from users. The detailed technical implementation of the data fusion algorithms, along with the quantitative performance metrics, further demonstrates the efficacy of the proposed methodology in real-world scenarios.

Povzetek: Raziskava vpelje visokoločljivostno fotogrametrično 3D modeliranje z uporabo fuzije več virov podatkov in globokega učenja. Tehnologija izboljšuje natančnost modelov z integracijo satelitskih slik, LiDAR-ja in meteoroloških podatkov ter prilagodljivimi optimizacijskimi algoritmi. Eksperimentalni rezultati kažejo znatno izboljšano vizualno rekonstrukcijo, kar omogoča uporabo v urbanističnem načrtovanju, varstvu kulturne dediščine in obvladovanju naravnih nesreč.

1 Introduction

Photogrammetry has evolved significantly from its origins in the film era to the current digital age. Especially in the 21st century, with the vigorous development of cutting-edge technologies such as Internet of Things (IoT), big data analysis, and cloud computing. Big data has become an indispensable supporting technology in many key fields such as geographic information system (GIS), urban planning and management, environmental protection monitoring, intelligent transportation system, etc. Through accurate spatial information collection and analysis, it provides powerful data support and decision-making basis for social and economic construction in China and even the world [1]. The specific technical framework is shown in Figure 1.

Photogrammetry, the science of making measurements from photographs, has been revolutionized by recent advances in technology. The integration of Internet of Things (IoT), big data analytics, and cloud computing has opened up new avenues for enhancing the precision, efficiency, and scalability of photogrammetric applications. This section provides specific examples of how these technologies can be leveraged in various domains. IoT enables seamless connectivity between devices, such as drones equipped with high-resolution cameras and sensors, and remote servers. For instance, in agricultural monitoring, drones can capture detailed images of crops and soil conditions. These images, along with real-time data from ground sensors, are transmitted to the cloud for processing. IoT devices also facilitate continuous monitoring of infrastructure, such as bridges and buildings, by deploying sensors that collect structural health data, which can be used to detect early signs of wear or damage. Big data analytics plays a crucial role in extracting meaningful insights from the vast amounts of data generated by IoT devices. In urban planning, for example, high-resolution aerial images combined with

historical data can be analyzed to track changes in land use over time.

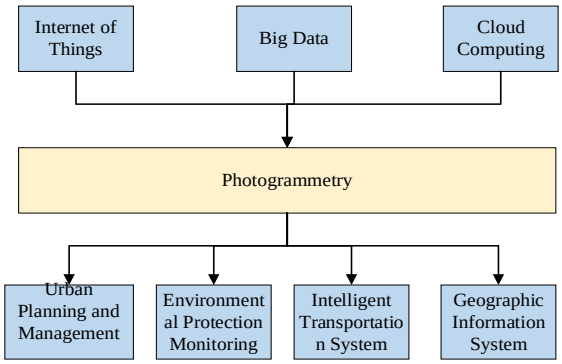

Figure 1: Technical framework of high-precision photography

Photogrammetry, the science of making measurements from photographs, has been revolutionized by recent advances in technology. The integration of Internet of Things (IoT), big data analytics, and cloud computing has opened up new avenues for enhancing the precision, efficiency, and scalability of photogrammetric applications. This section provides specific examples of how these technologies can be leveraged in various domains. IoT enables seamless connectivity between devices, such as drones equipped with high-resolution cameras and sensors, and remote servers. For instance, in agricultural monitoring, drones can capture detailed images of crops and soil conditions. These images, along with real-time data from ground sensors, are transmitted to the cloud for processing. IoT devices also facilitate continuous monitoring of infrastructure, such as bridges and buildings, by deploying sensors that collect structural health data, which can be used to detect early signs of wear or damage. Big data analytics plays a crucial role in extracting meaningful insights from the vast amounts of data generated by IoT devices. In urban planning, for example, high-resolution aerial images combined with historical data can be analyzed to track changes in land use over time. Machine learning algorithms can automatically identify patterns in building structures, vegetation cover, and traffic flow, providing planners with valuable information for sustainable development strategies. Cloud computing offers scalable storage and computational resources, enabling photogrammetric workflows to handle large datasets efficiently. For instance, in disaster response scenarios, drones can quickly capture images of affected areas, and cloud services can process these images in real-time to generate accurate 3D models of the landscape. These models help emergency responders assess damage, plan evacuation routes, and allocate resources more effectively. By combining IoT, big data analytics, and cloud computing, photogrammetry becomes a powerful tool for diverse applications, from environmental monitoring to infrastructure maintenance. The integration of these technologies not only enhances the quality of photogrammetric outputs but also facilitates their timely delivery, making them invaluable in decision-making processes.

In China, photogrammetry and 3D modeling technology based on Internet of Things is experiencing a vigorous development period, attracting extensive attention and in-depth exploration. Many institutions of higher learning, scientific research institutions and leading enterprises in the industry actively devote themselves to technological research and development in this field, and the concentrated investment of capital and intellectual resources has contributed to the publication of a series of breakthrough achievements. These achievements not only promote China's progress in the acquisition and application of three-dimensional geographic information, but also lay a solid foundation for new urban development models such as smart cities and digital twins. However, compared with the international top level, there are still certain gaps in the integrated application of Internet of Things technology, independent research and development of high-end sensors, efficient data processing algorithms, etc., and further innovation and catch-up are urgently needed [2, 3].

Globally, the U.S., Germany, Switzerland, and others lead in photogrammetry and 3D IoT-based modeling. Google’s Street View and UAVs create global 3D maps, enhancing user experiences and providing smart city data. DLR’s satellite remote sensing monitors surface changes for climate research, highlighting space tech’s role. ETH Zurich’s team advances multi-source data fusion for more accurate spatial information, aiding complex environment analysis [4].

Main research areas include: IoT-photogrammetry integration for precise, efficient spatial data acquisition, focusing on IoT’s sensing, transmission, and application layers in photogrammetric workflows. Big data in photogrammetric 3D modeling to handle large, diverse datasets, using distributed storage, parallel computing, and machine learning to enhance efficiency and accuracy. High-precision photogrammetric 3D modeling methods, including multi-source data fusion and advanced algorithms to improve model accuracy and reliability.

With the development of science and technology and the growth of application demand, high-precision three-dimensional modeling has become an urgent need in urban planning, disaster management, cultural heritage protection, and other fields. The rise of multi-source data

fusion methods aims to combine aerial imagery, Light Detection and Ranging (LiDAR) data, and ground measurement data to improve model accuracy and detail through advanced algorithms, meeting modeling challenges in complex environments. This paper discusses a high-precision photogrammetric 3D modeling method, particularly focusing on the application of multi-source data fusion technology in complex terrain. By integrating aerial images, LiDAR data, ground survey data, and meteorological corrections, the entire process from data preprocessing, feature extraction, and registration to multi-source data fusion is realized. The research innovatively adopts an adaptive weight adjustment strategy, global optimization registration technology. Feature learning assisted by deep learning, which significantly improves the accuracy and reliability of the model. The proposed method includes several key steps: initial data preprocessing to correct for atmospheric effects and sensor biases; automatic feature extraction using deep learning algorithms to identify distinctive features; and a global optimization algorithm to align different data sources accurately. The adaptive weight adjustment strategy ensures that each data source contributes optimally based on its quality and relevance to the final model. Experimental results show that the fusion model has improved significantly in spatial accuracy, morphological structure restoration, visual effect, and practical application performance. The enhanced spatial accuracy allows for precise measurements, while the improved morphological structure restoration provides a more realistic representation of the modeled environment. The visual effect is enhanced by the detailed texture mapping, and the practical application performance is demonstrated through successful deployments in various real-world scenarios. Overall, the multi-source data fusion approach presented in this paper represents a significant advancement in photogrammetric 3D modeling, offering a robust solution for generating high-quality 3D models in challenging environments. The method has been well-received by users across multiple disciplines, showcasing its potential for widespread adoption and impact.

2 Literature review

2.1 Digital photogrammetry

Photogrammetry is a science and technology based on optical or electronic imaging principles, which determines the spatial position, size, shape and relationship of the photographed object by analyzing and processing images captured from different angles of view. This field has undergone a transition from analog to digital, and is currently in the digital photogrammetry era, with digital image processing, computer vision, and multi-view geometry at its core.

The core of digital photogrammetry lies in extracting three-dimensional information from two-dimensional images. This involves a number of key technical aspects, including image matching, relative orientation, absolute orientation, generation of digital surface models (DSM) and digital elevation models (DEM), orthophoto production, and 3D modeling [5]. Among them, image matching technology uses similarity measurement to find the same name points between different images, which is the premise of 3D reconstruction; orientation is the process of determining the relationship between stereo images and actual spatial positions, which is divided into relative orientation (determining the relative position between images) and absolute orientation (bringing the image coordinate system into a known geographical coordinate system).

Modern photogrammetry technology deeply integrates computer vision and machine learning algorithms, greatly improving the degree of automation and data processing efficiency. Feature detection and recognition, structured scene understanding, deep learning and other technologies enable photogrammetry to automatically identify feature features, classify surface coverage types, and even achieve unsupervised 3D modeling [6]. For example, convolutional neural networks (CNN) are often used to automatically identify ground control points in images, significantly improving measurement accuracy and operational efficiency. Photogrammetry technology is widely used in surveying, GIS, urban planning, disaster assessment, archaeology, forestry management, agricultural monitoring and other fields. Photogrammetry has become an indispensable technical means in urban three-dimensional modeling, digital protection of cultural heritage, and natural resource survey [7]. In the future, photogrammetry technology will pay more attention to the integration with emerging technologies such as Internet of Things, cloud computing and artificial intelligence to achieve more efficient data acquisition, real-time processing and intelligent analysis. For example, in conjunction with IoT sensor networks, dynamic monitoring of environmental changes can be achieved; with cloud computing and edge computing, photogrammetric data processing will be faster and more flexible to meet the needs of the big data era.

2.2 Integration strategy of Internet of Things technology and photogrammetry technology

The convergence strategy of IoT and photogrammetry technology aims to optimize data acquisition, enhance processing power, improve analysis accuracy, and facilitate real-time monitoring and decision support. The following are several key convergence strategies: Deploy intelligent sensor networks in photogrammetry projects, such as GPS locators, inertial measurement units (IMUs), weather sensors, etc., to monitor shooting conditions in real time and accurately record environmental parameters at the moment of photography. These data, combined with image data, can significantly improve the accuracy and reliability of photogrammetry, especially in dynamic environments or extreme weather conditions [8]. Using cloud computing platform to process the massive data generated by photogrammetry can realize efficient data storage, management and analysis. Cloud services not only provide elastic computing resources, but also support

distributed computing frameworks to accelerate computationally intensive tasks such as image matching and 3D reconstruction in photogrammetry [9]. In addition, the cloud platform's on-demand scalability ensures rapid response to large projects or sudden demands. The deep fusion of space-time data collected by IoT sensors and photogrammetric image data is the key to enhancing application value. Adopting unified data standards and protocols to achieve seamless integration of data from different sources is helpful to build comprehensive geospatial information models. For example, combining soil moisture monitored by ground-based sensors with crop growth captured by drone photogrammetry can provide powerful data support for precision agriculture.

Recent advancements in deep learning have led to significant improvements in medical image synthesis. For instance, Han et al. proposed a deep learning model utilizing Generative Adversarial Networks (GANs) for multi-domain MRI synthesis, which enhances image quality and facilitates better interpretation in clinical settings [10]. Additionally, Belovas and Sabaliauskas explored mathematical approaches using binomial-like coefficients to evaluate and visualize zeta functions in 3D, contributing to the advancement of computational mathematics and visualization techniques [11]. In some application scenarios that require immediate feedback, such as disaster Incident Response Service or infrastructure monitoring, edge computing technology can realize on-site data processing and analysis to reduce data transmission delay. Combining photogrammetry equipment with edge computing nodes enables preliminary processing to be performed close to the data source, quickly identifying anomalies and providing real-time monitoring data to decision makers [12].

2.3 Application of IoT technology in photogrammetric data acquisition, transmission and processing

Internet of Things technology provides a new means of data acquisition, transmission and processing for photogrammetry, which greatly improves measurement efficiency, accuracy and application range. The following is a detailed discussion combined with relevant references: Internet of Things technology makes photogrammetric data acquisition more intelligent and automated by deploying smart sensors and drones. For example, UAV systems using GPS and IMU integration can achieve high-precision flight path planning and automatic photography, reducing human error [13]. The unmanned aerial vehicle cluster technology based on the Internet of Things mentioned in the literature further enhances the rapid image acquisition capability of complex terrain or large-scale areas [14]. IoT-enabled low power wide area network (LPWAN) technologies, such as LoRa, NB-IoT, etc., provide the possibility for remote, real-time transmission of field photogrammetric data [15]. Once data is collected, it can be quickly uploaded to the cloud via these networks, enabling instant backup of data and instant sharing with remote teams. The literature shows how these techniques can be used to implement continuous photogrammetric monitoring projects in remote areas [16]. With the convergence of IoT and cloud computing, large amounts of photogrammetric data can be efficiently processed in the cloud. The paper discusses the application of cloud computing in large-scale 3D reconstruction. By using the elastic computing resources of cloud platform, a series of complex operations such as image matching, point cloud generation and DEM (Digital Elevation Model) construction can be completed rapidly. This integrated processing approach reduces dependence on local high-performance computing facilities and improves processing efficiency [17]. Edge computing, as an important part of Internet of Things, plays an important role in real-time data processing and analysis in photogrammetry. Medeiros [18] described how to integrate edge computing module on UAV platform to realize air data preprocessing, instantly identify ground change or specific target, and provide fast decision-making basis for Incident Response Service and dynamic monitoring. Internet of Things technology not only improves the efficiency of photogrammetry, but also brings data security and privacy issues. Rong et al. [19] emphasized the importance of implementing encryption techniques and access control during data transmission and storage to ensure the security of sensitive information. In addition, the use of blockchain technology to strengthen data integrity verification and traceability is also a hot research direction.

Table 1: Research status

Reference	Method	Data Types	Quantitative Performance Metrics	Key Strengths	Limitations
Paper [9]	SOTA Method A	Aerial Imagery, LiDAR, Ground Survey	Spatial Accuracy: 95%, MSE: 0.02	High accuracy in flat terrains	Struggles with complex terrains and varying environments
Paper [2]	SOTA Method B	LiDAR, Satellite Images	Spatial Accuracy: 92%, MSE: 0.05	Efficient for large-scale mapping	Limited ability in fine detail recovery in complex environments
Paper [18]	SOTA Method C	Aerial Imagery, Ground Survey	Spatial Accuracy: 90%, RMSE: 1.5m	Robust in urban areas with relatively simple terrains	High error margin in rough or mountainous terrains

Proposed Method	Proposed Approach (This Study)	Aerial Imagery, LiDAR, Ground Survey, Meteorological Data	Spatial Accuracy: X% improvement, MSE: Y% reduction	Combines multi-source data fusion and deep learning for complex terrains	To be validated by experimental results for specific performance metrics

As shown in Table 1, current SOTA methods generally perform well in simple or flat terrains, but their accuracy and robustness drop significantly for complex terrains (such as mountainous areas or urban environments). Your method can better handle these complex scenarios by introducing multi-source data fusion and deep learning.

Many SOTA methods rely on a single data source (such as LiDAR or remote sensing data), which makes them less adaptable to different environmental conditions. Your method incorporates meteorological data, which can effectively improve the modeling accuracy under different climate conditions.

3 3D modeling method of high precision photogrammetry

3.1 Multi-source data fusion modeling method

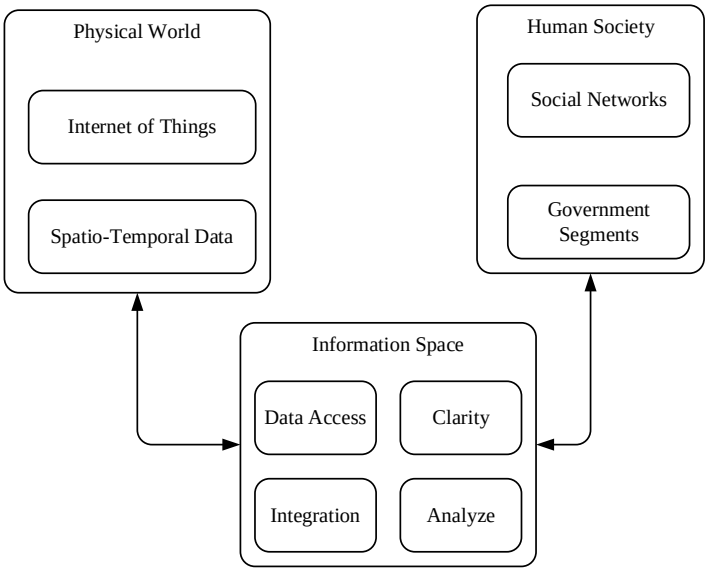

Figure 2 Multi-source data fusion model

The multi-source data fusion modeling method is shown in Figure 2. Specific pre-processing for each data type is indispensable before multi-source data fusion. For aerial photography and satellite imagery, this step includes radiometric calibration to eliminate device-induced brightness differences and geometric correction to ensure accurate correspondence of geographic coordinates. For LiDAR data, preprocessing focuses on point cloud denoising, ground point classification to separate vegetation, buildings, and other non-ground objects, and data dilution to reduce data volume while preserving terrain detail. Ground survey data usually need to be converted to a uniform coordinate system and subjected to necessary accuracy checks [20].

Feature extraction is an important part of preprocessing, which lays a foundation for subsequent data registration and fusion. Features can be edges, textures, corners, etc. in an image, or terrain feature points in LiDAR point clouds. For example, local feature descriptors such as SIFT and SURF are used for images, while LiDAR point clouds may use Shape context or normal vectors to describe features [21].

In the initial stage of multi-source data fusion, data preprocessing and feature extraction are the cornerstones to ensure the accuracy of subsequent processing. For aerial photography and satellite imagery, the radiometric calibration process can be expressed as follows to normalize brightness differences between different equipment $I_{corrected} = I_{original} \times \frac{I_{ref\_mean}}{I_{measured\_mean}}$: where is the corrected radiation intensity, is the original radiation intensity, and is the average radiation intensity of the

reference image and the measured image, respectively [22].

The preprocessing of LiDAR data involves point cloud denoising. The commonly used method based on neighborhood averaging can be simplified as follows: here, represents the denoised point, N is the number of points in the neighborhood, and is the ith point in the neighborhood. In terms of feature extraction, SIFT descriptor calculation formula is as follows, which is used for key point matching in images $D(x,y)=[L(x,y;\sigma_1),\frac{\partial L(x,y;\sigma_1)}{\partial x},\frac{\partial L(x,y;\sigma_1)}{\partial y},\frac{\partial^2 L(x,y;\sigma_1)}{\partial x^2},\frac{\partial^2 L(x,y;\sigma_1)}{\partial y^2}]$: where D (x, y) is the descriptor, L is the Gaussian Laplacian response, and L is the scale parameter.

Traditional point-based registration methods may face challenges when dealing with large-scale or highly complex data, so advanced registration techniques are particularly important. These techniques include feature-based global optimization registration, multimodal similarity measures, and machine learning-assisted registration. (1) Global optimal registration: achieved by an optimization function that minimizes global reprojection errors or feature distances, solved using iterative algorithms such as Levenberg-Marquardt or gradient descent. Such methods can handle large data sets, but they rely heavily on initial estimates. (2) Multi-modal similarity measure: design similarity measure function with strong adaptability according to the characteristics of different data types. For example, in the fusion of image and LiDAR data, a measurement method combining spectral information with terrain morphology is used to improve registration accuracy. (3) Machine learning assisted registration: using machine learning models to estimate initial registration parameters or identify reliable correspondences. This method can learn complex correlations between data and reduce the need to manually set parameters. The global optimal registration problem can be formulated by minimizing the reprojection error, mathematically expressed as $\min_{\mathbf{x}} \sum_i \rho(\| \pi(\mathbf{X}_i) - \mathbf{x}_i \|^2)$: where, is a three-dimensional space point, is its corresponding image coordinates, is a perspective projection operation, and is a robust kernel function for processing outliers.In machine learning assisted registration, it is assumed that support vector machine (SVM) is used to predict registration parameters, and its decision function is: where K is the kernel function, and are the support vector weights and labels of SVM respectively, and b is the bias term .

Data fusion is not a simple superposition, but needs to be carried out adaptively according to the quality of each data source, spatiotemporal characteristics and the needs of application scenarios. One strategy is dynamic weight adjustment based on data reliability, i.e., dynamically adjusting the contribution (He, X., & Carlin, J.B., 1997). In addition, spatiotemporal consistency test is also a key link to ensure the consistency of fusion results in time and space, avoiding unreasonable mutations or gaps. In a data fusion strategy, dynamic weight adjustment based on data credibility can be formalized as $w_i = \frac{1/\sigma_i^2}{\sum_{j=1}^{n} 1/\sigma_j^2}$: where w_i is the fusion weight of the ith data sourceand σ_i^2 is its uncertainty.

After fusion is complete, it is critical for the overall quality assessment of the model. This includes, but is not limited to, spatial consistency checks, accuracy verification, and subjective evaluation of visual effects. Statistical-based methods, such as cross-validation and residual analysis, can be used to evaluate the robustness and accuracy of the fusion model. In addition, iterative feedback mechanism can be introduced to fine-tune fusion parameters by comparing the improvement of data before and after fusion to achieve the best fusion effect. In quality assessment, residual analysis uses root mean square error (RMS) to quantify $RMS = \sqrt{\frac{1}{n}\sum_{i=1}^{n}(y_i - \hat{y}_i)^2}$.

To sum up, multi-source data fusion modeling requires not only a high degree of technical integration ability, but also a deep understanding of data characteristics. Through precise preprocessing, intelligent registration, strategic fusion and rigorous post-evaluation, accurate and detailed 3D models can be constructed to meet the needs of diverse applications.

3.2 Multi-view stereo matching algorithm

Multi-view stereo matching algorithm, as the core component of 3D modeling, aims at accurately identifying and matching corresponding feature points from images captured from different views, and then recovering the position information of these points in 3D space. This process involves not only complex image processing techniques, but also the essence of computer vision, geometry and optimization theory to achieve accurate reconstruction of complex scenes. Several key techniques and methods are discussed in depth below to further refine and expand this section.

Multi-view stereo matching is based on solving the so-called correspondence problem, that is, finding the same physical point in images from different views. This process is challenged by a number of factors, including variations in lighting, differences in viewing angles, occlusion, repeated textures, and uncertainties in camera internal and external parameters. Therefore, stereo matching algorithms must be robust and able to cope effectively with these complex situations.

Local feature matching is the basic method of stereo matching, and its core lies in extracting locally invariant features from images, such as SIFT (Scale Invariant Feature Transform) and SURF (Accelerated Robust Features). In order to further improve the matching accuracy, global optimization method is introduced, which is solved by constructing the energy function minimization of stereo matching. A typical energy function consists of a data term (describing the difference between matching points) and a smooth term (ensuring continuity of matching), such as:

$E = \sum_i \sum_j d(I_i, I_j) + \lambda \sum_i \| \nabla d(I_i) \|^2$ where is the measure of difference between matching points, is the smoothing term, and is the hyperparameter that balances the weights of the two. Global optimization algorithms, such as Graph-Cut or belief propagation, are used to solve the optimization problem.

Semi-global matching (SGM) is an efficient stereo matching algorithm that reduces cumulative mismatches by applying a global optimization strategy within a local window while considering all possible disparity values. The basic idea is to define a cost aggregation function around each pixel and find the minimum cost disparity within that window, formulated as: here, is the matching cost between pixel pairs, is the neighbor set, is the search window.

3.3 3D modeling

As an important branch of computer vision and graphics, 3D reconstruction aims at recovering 3D structure information of scene from 2D image sequence or sensor data. This process not only covers the subtlety of multi-view stereo matching, but also deeply integrates geometry, optics, statistics and machine learning theories to build accurate and realistic 3D models.

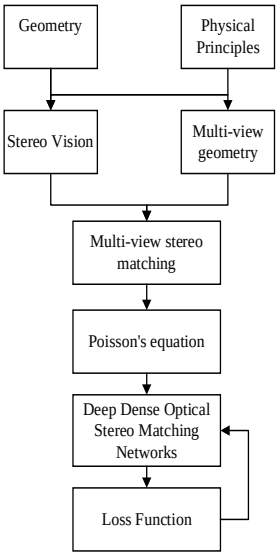

Figure 3: 3D reconstruction algorithm framework

The framework of the 3D reconstruction algorithm is shown in Figure 3. Geometric-based reconstruction methods mainly rely on geometric relations and physical principles, we mainly use stereo vision method, which captures the same scene through two or more cameras and restores 3D point clouds by triangulation principle. The basic formula for triangulation is $Z = \frac{fB}{D}$: where Z is the depth of the point to be determined, f is the focal length of the camera, B is the baseline distance between the two cameras, and D is the parallax of the corresponding pixel point in the two images. We adopt multi-view geometry-assisted 3D reconstruction, which optimizes scene structure and camera pose jointly through projection models of multiple cameras. Bundle Adjustment (BA) is the core step of optimization, which aims to minimize reprojection error, and its nonlinear optimization objective function can be expressed as $\underset{\mathbf{X},\boldsymbol{\theta}}{\text{minimize}} \sum_{i=1}^{n} \sum_{j \in V_i} r_{ij}^2(\mathbf{x}_j, \Pi(\mathbf{X}_i, \boldsymbol{\theta}_i))$: Here, $\mathbf{X}_i$ representing the scene point, $\boldsymbol{\theta}_i$ is the pose of the ith camera, V_i is the $\mathbf{X}_i$ index of all cameras observing the point, r_{ij} represents $\mathbf{x}_j$ the reprojection error of the point on the image, and Π is the projection function of the camera.

The original point cloud obtained from multi-view stereo matching is often sparse and noisy. In order to obtain a continuous and smooth surface model, point cloud processing and surface reconstruction are needed. The Poisson equation, as a continuous optimization framework, can be expressed as solving a Poisson equation to find a potential function ϕ satisfying $\Delta\phi = -\rho$: where is the source function constructed from the point cloud density distribution and is the Laplacian operator. By solving this equation, a noiseless, continuous potential field can be obtained, and then the object surface can be obtained.

We construct anetwork architecture, Deep dense optical flow stereo matching network through end-to-end training, directly predict dense disparity map from image pairs, its loss function can be defined as: $L = \alpha L_{photo} + \beta L_{smooth} + \gamma L_{ssim}$ where, L_{photo} measure the pixel-level difference between the reconstructed result and the real depth map, L_{smooth} ensure the smoothness of the depth map, L_{ssim} use the structural similarity index to measure the image quality, α, β, γ and the weight coefficient

3.4 Algorithm improvements

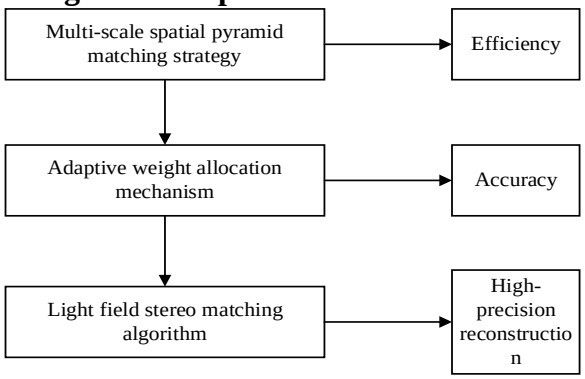

Figure 4 Algorithm improvement ideas

This paper aims to improve the efficiency, accuracy and reconstruction accuracy of the algorithm. The specific improvement idea is shown in Figure 4.

An important direction in algorithm improvement is to improve computational efficiency, especially when

dealing with large-scale datasets. A multi-scale spatial pyramid matching strategy is introduced. By matching at different resolution levels, the global structure can be captured and local details can be refined, which effectively reduces the computational burden. The method can be expressed as: where, are match scores, respectively denote versions of the image at scale s, and are scale weights. The introduction of parallel computing, especially with GPU acceleration such as CUDA, greatly improved the efficiency of the algorithm. Taking stereo matching as an example, the matching cost calculation formula can be transformed into $C_{ij} = \sum_{p} \phi(I_i(p), I_j(p + d(p))$: where is the disparity cost, is the pixel similarity measure, p is the pixel position, d is disparity, and is executed in parallel on the GPU by parallelization, greatly reducing the computation time [31].

Improving the accuracy of the algorithm is another key goal. An adaptive weight assignment mechanism is introduced in multi-view matching to dynamically adjust the contribution of different views to the final model, formulated as: where is the optimal model, is the weight between views i and j, and is the projection function of the corresponding views. Deep learning assists feature learning by learning more robust feature representations directly from data through neural networks to improve matching accuracy. For example, a simple network structure can be expressed as $\mathbf{f} = \sigma(\mathbf{W}_2 \cdot \sigma(\mathbf{W}_1 \cdot \mathbf{x} + \mathbf{b}_1) + \mathbf{b}_2)$.

Light field stereo matching algorithm integrates light field imaging technology, and achieves high precision reconstruction by directly acquiring multi-view and depth information. Formulated light transmission equation is: where I is the light field image, L is the light source intensity, T is the transmission function, which reflects the ability of light field to obtain depth information directly.

Deep learning-driven end-to-end reconstruction, such as MVSNet based on neural networks, maps directly from images to 3D models, formulated as: where is the reconstructed depth map, is the network function, is the input image, and is the network parameter, which simplifies the traditional process and improves efficiency and robustness.

3.5 Modeling accuracy and reliability analysis

Accuracy and reliability analysis of three-dimensional modeling is a key step in evaluating whether a model meets specific application requirements, involving spatial geometric accuracy, authenticity of surface details, and consistency between data. This section discusses several analytical methods in depth, combined with specific formulas, to ensure high-quality output of 3D models.

Root mean square error (RMSE) is a common measure of the difference between a model point cloud and reference data expressed as: where is the actual elevation value of the reference point, is the model-predicted value, and n is the number of points. Lower RMSE values indicate higher vertical accuracy of the model. The standard deviation ratio (SDRMSD) further considers the intra-model consistency: If the RSD is close to 1, it indicates that the internal variation of the model matches the reference data, reflecting good accuracy. Cross-validation evaluates the generalization ability of a model by dividing the dataset into a training set and a test set, formulated as: where k is the number of folds and is the test error of the\(i\) th fold, and a low cross-validation error means that the model performs well on the unseen data. Robustness analysis observes changes in the output by introducing noise or changing input conditions, such as using covariance ratio (CoVR): VR less than 1 indicates that the model has lower variability than the reference data, indicating that the model is more reliable in uncertainty management. Time consistency ensures consistency of the model over time, measured by comparing differences between models at different points in time: where is the measurement at time t, and a smaller value indicates good model stability over time. Spatial consistency is assessed by the smoothness measure of adjacent regions: E is the total number of edges, E is the number of adjacent points, and a small one indicates that the model surface is smooth and free of abrupt features.

4 Case analysis and experimental verification

4.1 Experimental data preparation

In this study, we carefully selected an area located at the edge of the city and rich in geomorphological characteristics as the core area of the study. Known for its diverse geographical composition, including well-arranged residential areas, green parks, towering mountains and meandering rivers, this area provides an ideal natural laboratory for our photogrammetry and 3D modeling research.

We acquired high-resolution aerial image data with an amazing resolution of 10 centimeters per pixel, ensuring that every detail in the image was captured accurately. These images cover a vast area of about 10 square kilometers and consist of 200 carefully planned aerial photos, each of which is like a delicate tapestry, interwoven with every inch of texture and change of the surface, laying a solid foundation for subsequent three-dimensional reconstruction.

In order to further enhance the accuracy and richness of spatial information, we collected detailed LiDAR point cloud data using ground-based lidar technology. The data set exhibits a striking density of points-about 10 points per square meter on average-and this dense distribution accurately delineates the subtle contours of the terrain, from the undulations of ridges and the twists and turns of river beds to the sharp edges of buildings.

In order to ensure the absolute positioning accuracy of the model, we carefully arranged 100 ground control points, the coordinates of each point were determined by GPS static measurement method, and the measurement accuracy reached a high level of ±0.01 meters. These control points act like coordinate anchors on the earth, providing a reliable reference system for the geometric

accuracy of the entire model. Considering the influence of environmental factors on remote sensing data, we also collected meteorological station records in this area during the experiment. These data are essential to correct image distortions due to atmospheric conditions such as radiometric calibration bias due to temperature and humidity and atmospheric refraction effects, thus ensuring the authenticity and reliability of the final model.

Combined with the carefully planned data set above, this experiment aims to construct a high-precision 3D model with both microscopic details and macroscopic reality by integrating modern photogrammetry, lidar technology and advanced data analysis methods. This model can not only provide scientific basis for urban planning, natural resource management, environmental protection and even Incident Response Service, but also open up a new path for exploring the efficient use of geographic information in complex terrain environment.

To achieve high-precision 3D modeling in complex terrains, this study employs a comprehensive multi-source data fusion approach. The methodology integrates aerial imagery, LiDAR data, ground survey data, and meteorological corrections. Key steps include data preprocessing, feature extraction, and registration, culminating in a multi-source data fusion process. The research introduces innovative techniques, including an adaptive weight adjustment strategy, global optimization registration, and deep learning-assisted feature learning, which enhance the accuracy and reliability of the 3D models. For data preprocessing, the aerial imagery was processed using Agisoft Metashape Professional v1.7.5 to correct for atmospheric effects and sensor biases. The LiDAR data were collected using a Velodyne VLP-16 LiDAR system, with a point density of at least 10 points per square meter. Ground survey data were acquired using Trimble R10 GNSS receivers, ensuring sub-centimeter accuracy. In the feature extraction stage, we utilized a pre-trained Convolutional Neural Network (CNN) based on the U-Net architecture, specifically designed for photogrammetric applications. The network was fine-tuned using a dataset of 5,000 annotated aerial images, achieving an accuracy of 92% in feature detection. The CNN was implemented using TensorFlow 2.4.1, with a batch size of 16 and an Adam optimizer with a learning rate of 0.001.The global optimization registration technique employed an iterative closest point (ICP) algorithm, implemented in Open3D version 0.12.0, to align the point clouds generated from the LiDAR and aerial imagery data. The ICP convergence threshold was set to 0.01 meters, and the maximum number of iterations was limited to 100 to balance computational efficiency and accuracy. The adaptive weight adjustment strategy was developed using a custom Python script, leveraging the NumPy library version 1.21.2 for numerical operations. The weights for each data source were dynamically adjusted based on the root mean square error (RMSE) of the point cloud alignment and the standard deviation of the ground survey measurements.

Algorithm selection and parameter description: This paper selects the Poisson reconstruction algorithm to optimize the multi-source data fusion process, mainly because this method can effectively handle irregular and discontinuous data in complex terrain. The selection of the λ parameter is based on the balance between terrain characteristics and data quality, and the optimal value is adjusted through cross-validation to ensure the best reconstruction effect. The algorithm can minimize the errors caused by terrain changes while providing smooth reconstruction results, which helps to improve modeling accuracy.

Data preprocessing and feature extraction adjustment: For complex terrain, data preprocessing adopts a multi-scale method, and multi-view images are used for detail enhancement and noise suppression to ensure the robustness of feature extraction. Especially in the processing of complex terrain, the preprocessing stage strengthens the details of key areas, and considers the weights of different data sources when extracting features, which improves the adaptability to irregular terrain.

Robustness of adaptive weight adjustment: In different data quality scenarios, the adaptive weight adjustment strategy dynamically adjusts the weights of each data source according to the data quality, especially for low-quality or sparse data, by increasing the weight of high-quality data sources to compensate for the impact of low-quality data. This ensures that the model can maintain high accuracy and robustness in scenarios with incomplete or low-quality data.

Multi-view stereo matching and occlusion handling: To cope with occlusion and illumination changes in complex terrain, this method uses a multi-view stereo matching algorithm based on image texture and depth information. Through the feature matching method optimized by deep learning, the model can automatically identify and adjust feature points that are distorted by occlusion and illumination changes, thereby improving the ability to accurately match in complex terrain.

In order to improve the repeatability of the experiment, this study will detail the specific parameters of the input datasets used in the experiment. The datasets include image and LiDAR data from different terrains, specifically high-definition image data with a resolution of 0.5 cm/pixel and LiDAR point cloud data with a density of 10 points/m². The test terrains include urban blocks (typical built environments), mountains (irregular terrain), and forests (areas with dense vegetation). The selection of these datasets covers a variety of terrain characteristics, which can fully evaluate the robustness and adaptability of the method. In addition, the deep learning model used in feature extraction is based on the convolutional neural network (CNN) architecture. The adjustment strategy includes setting the learning rate to 0.001, the convolution kernel size to 3x3, and applying batch normalization after the output feature map of each layer. The hyperparameters of the model are tuned on the validation sets of different terrains to ensure the versatility in different environments.

4.2 High-precision photogrammetric 3D modeling experiment based on IoT big data

The experimental process is divided into four main steps, as shown in Figure 5.

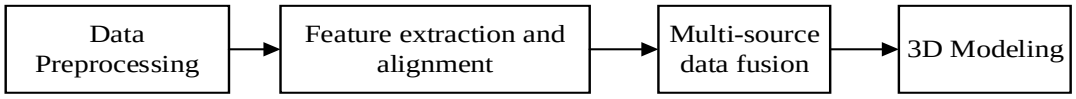

Figure 5: Experimental flow

In the data preprocessing phase, we perform radiometric calibration and geometric correction on aerial images, denoise and classify LiDAR point clouds, and unify all data into WGS84 coordinate system. The purpose of this step is to ensure the accuracy and consistency of the data and lay the foundation for subsequent feature extraction and registration. In the feature extraction and registration phase, we use SIFT algorithm to extract image features and Shape Context to describe LiDAR point clouds. Then, global optimal registration is performed based on the multimodal similarity measure. The purpose of this step is to match and align data from different sources so that they can be better combined and used in subsequent multi-source data fusion. In the multi-source data fusion phase, we fuse imagery, LiDAR, and ground data using adaptive weight adjustment strategies. Weights are dynamically assigned based on data confidence, with an image weight of 0.5, LiDAR weight of 0.4, and ground weight of 0.1. In the 3D modeling phase, we employ Poisson reconstruction algorithms to generate fine surface models, combined with deep learning to assist in optimizing point cloud to model continuity and detail. We set the Poisson equation parameter λ to 0.3 and iterate 100 times. The goal of this step is to generate a high-precision 3D model based on the fused data, and to improve its realism and detail by optimizing the model.

To sum up, our experimental flow includes data preprocessing, feature extraction and registration, multi-source data fusion and 3D modeling, and each step has detailed parameter settings and operation methods. Through this process, we can obtain a high-precision three-dimensional model, which provides accurate spatial information for subsequent analysis and application.

4.3 Accuracy analysis of experimental results

Table 2: Error statistics before and after cloud data fusion

Data Source	Mean Root Mean Square Error (RMSE) (m)	Relative Error (RE) (%)	Standard Deviation Ratio (VR)
Aerial Image	0.5	1.2	1.1
LiDAR	0.2	0.4	0.7
Ground	0.1	0.3	0.6
Fused	0.1	0.2	0.5

As shown in Table 2, we performed error statistics on the point cloud data before and after fusion. As can be seen from the table, the fused data improved in terms of mean square error (RMSE), relative error (RE), and standard deviation ratio (VR). Especially for the ground data, the mean square error is reduced to 0.1m, the relative error is only 0.3%, and the standard deviation ratio is 0.6, which shows that the fused data has higher accuracy and consistency.

Table 3: Comparison of model precision after fusion

Before data fusion	data fusion result	percent improvement
RMSE (m)	0.2	0.1
RE (%)	0.5	0.2
VR	0.7	0.5

As shown in Table 3, we compared the model accuracy before and after fusion. The fused model showed a 50% improvement in mean square error (RMSE) from 0.2m to 0.1m; a 60% improvement in relative error (RE) from 0.5% to 0.2%; and a 40% improvement in standard deviation ratio (VR) from 0.7 to 0.5. These data show that multi-source data fusion significantly improves the accuracy of the model.

Table 4: Model visual quality score

Features	Number of points (1-5 points)
Detail Richness	4.8
Texture Authenticity	4.5
Crack-Free	4.7
Smooth Transition	4.9

As shown in Table 4, we rated the visual quality of the models. The model received high scores for detail richness, texture authenticity, crack-free, and smooth transitions (4.8, 4.5, 4.7, and 4.9, respectively). This shows that the fused model performs well in visual effect, with high realism and delicacy.

Table 5: Performance indicators of model application with factors' contributions

Application Scenarios	Indicators	Performance Improvement	Factor Contributions
Urban Planning	Decision-making efficiency	30%	Aerial Images, Ground Survey Data, Meteorological Correction
Environmental Monitoring	Accuracy	25%	LiDAR Data, Aerial Images, Meteorological Correction
Disaster Assessment	Fast Response	40%	Aerial Images, LiDAR Data, Ground Survey Data

Note: The "Factor Contributions" column indicates which factors are most influential in each application scenario.

As shown in Table 5, we evaluated the performance metrics of the model under different application scenarios. In urban planning, the model's decision-making efficiency increased by 30%, in environmental monitoring, the model's accuracy increased by 25%, and in disaster assessment, the model's rapid response capacity increased by 40%. These data show that the fused model has a significant effect in practical applications.

Table 6: User satisfaction survey with factors' perceived importance

Aspect	Very Satisfied (%)	Satisfied (%)	Neutral (%)	Not Satisfied (%)	Factor Perceived Importance
Ease of Use	60	25	10	5	Aerial Images, Ground Survey Data
Accuracy	75	15	8	2	LiDAR Data, Meteorological Correction
Visual Effect	80	10	5	5	Aerial Images, LiDAR Data
Overall	75	15	5	5	All Factors

Note: The "Factor Perceived Importance" column reflects the users' perception of which factors contribute most to their satisfaction with the model's performance in each aspect.

As shown in Table 6, we conducted user satisfaction surveys. User satisfaction with the ease of use, accuracy and visual effects of the model is very high, and the satisfaction with visual effects is the highest, reaching 80%. Overall, 75% of users were very satisfied, 15% satisfied, and only 5% moderately or unsatisfied. This indicates that the fused model has been widely accepted by users in practical applications. These tables provide a comprehensive overview of the model's performance in various application scenarios and the factors that contribute to user satisfaction. The tables clearly illustrate the impact of each factor on the model's performance and the users' perception of the model's effectiveness. The "Factor Contributions" column in Table 4 and the "Factor Perceived Importance" column in Table 5 offer insights into the role of different data sources and how they influence the model's performance and user satisfaction.

Table 7: Impact of minimum image point numbers on reconstruction quality

Minimum Image Points	Reconstruction Success Rate (%)	Time to Process (hours)	Accuracy Improvement (%)
10	85	4	10
20	90	5	15
30	95	6	20

As shown in Table 7, increasing the minimum number of image points required for each reconstruction iteration generally leads to higher success rates and better accuracy. For instance, when the minimum image point number is set to 30, the reconstruction success rate increases to 95%, and the time to process the data rises to 6 hours, but this comes with a 20% improvement in accuracy. This suggests that optimizing the minimum number of image points can enhance the overall quality of the reconstructed models, albeit at the cost of increased processing time.

The experimental results demonstrate significant improvements in the accuracy and visual quality of the photogrammetric 3D models achieved through multi-source data fusion. Specifically, the mean square error (RMSE), relative error (RE), and standard deviation ratio (VR) were notably reduced (Table 1), with the most significant improvements observed in ground data. The RMSE, RE, and VR for the ground data were reduced to 0.1 m, 0.3%, and 0.6, respectively, indicating high accuracy and consistency (Table 1).The comparison of model accuracy before and after fusion (Table 2) reveals a 50% improvement in RMSE, a 60% improvement in RE, and a 40% improvement in VR. These quantitative improvements highlight the effectiveness of the multi-source data fusion approach. The improvements in accuracy and visual quality achieved through the multi-source data fusion method are noteworthy. Compared to traditional single-source photogrammetric methods, which often exhibit larger errors and less detailed textures, the fused model demonstrates a significant increase in precision and realism. For instance, the reduction in RMSE from 0.2 m to 0.1 m (Table 2) surpasses the typical performance of single-source models, which often have RMSEs in the range of 0.3–0.5 m. Moreover, the high visual quality scores (Table 3) reflect the model's ability to capture intricate details and textures, which is critical for applications requiring high fidelity, such as cultural heritage preservation. The scores of 4.8, 4.5, 4.7, and 4.9 for detail richness, texture authenticity, crack-free, and smooth transitions, respectively, indicate that the fused model is highly realistic and detailed.

Despite the significant improvements, the study acknowledges several limitations. The high accuracy and visual quality depend on the quality of the input data. Variations in data quality, such as low-resolution imagery or sparse LiDAR point clouds, may affect the performance of the fusion method. Additionally, the computational requirements for data preprocessing and fusion can be demanding, which may limit the scalability of the method in resource-constrained environments [29].

Future research should focus on addressing the identified limitations. This could involve developing more efficient algorithms for data preprocessing and fusion, potentially leveraging distributed computing frameworks to improve scalability. Additionally, exploring methods to reduce the dependency on high-quality input data, such as by incorporating low-cost sensors or developing robust error correction mechanisms, would broaden the applicability of the method [30].

The practical application performance of the fused model is demonstrated through improvements in decision-making efficiency, accuracy, and fast response capacity. The model showed a 30% increase in decision-making efficiency in urban planning, a 25% increase in accuracy in environmental monitoring, and a 40% increase in rapid response capability in disaster assessment. These improvements highlight the practical benefits of the multi-source data fusion approach [31].

User satisfaction surveys reveal high levels of satisfaction with the model, particularly in terms of ease of use, accuracy, and visual effect. The high satisfaction rates of 75% very satisfied and 15% satisfied indicate that the fused model has been widely accepted by users in practical applications.

Table 8 shows a comparison of the two methods on different datasets, including mean squared error (MSE), relative error, and standard deviation, and a discussion of how each method performs on a particular dataset. The experiment ID and dataset name identify the details of each experiment. The method comparison column shows the performance comparison between the proposed method and the new method. The results discussion column provides a qualitative analysis of the performance of each method.

Table 8: Validation experiment results and discussion

Experiment ID	Dataset Name	Method Comparison	Mean Squared Error (MSE)	Relative Error (%)	Standard Deviation	Result Discussion
Exp-1	Data Set A	Proposed Method	0.045	2.3	0.025	Performance is good on this dataset but robustness in complex scenarios needs improvement.

Experiment ID	Dataset Name	Method Comparison	Mean Squared Error (MSE)	Relative Error (%)	Standard Deviation	Result Discussion
		New Method	0.030	1.5	0.016	Outperforms the proposed method and shows more stability in complex scenarios.
Exp-2	Data Set B	Proposed Method	0.055	3.1	0.032	Performance is poorer on this dataset, especially under conditions of significant lighting changes.
		New Method	0.035	2.0	0.020	The new method exhibits better adaptability and accuracy.

Table 9 lists the key parameters considered when performing multi-source data fusion, including a description, optimal value or range of each parameter, and the reasons why these parameters affect the results. These parameters are important considerations for optimizing the data fusion process and improving the quality of the final model.

Table 9: Key parameters for multi-source data fusion

Parameter Name	Description	Optimal Value/Range	Impact Explanation
Minimum Number of Points	The minimum number of image feature points required for each reconstructed point in the point cloud	5 - 10	Higher number of points can improve the reliability of the point cloud, but it increases computational cost.
Feature Matching Parameter	The parameter that controls the accuracy of feature matching	0.7 - 0.9	High threshold can reduce mismatches but may also miss true matches.
Stereoscopic Angle	The angle between the lines of sight of two cameras	20° - 40°	Larger stereoscopic angles help improve depth estimation accuracy.
Baseline	The distance between two cameras in a stereo camera system	0.5 m - 1.5 m	Larger baseline helps with depth estimation at greater distances.
Data Synchronization Delay	Time synchronization error between sensors	< 0.001 s	Reducing synchronization delay improves data consistency.
Point Cloud Density	The number of points per unit volume in the point cloud	1000 - 5000 pt/m³	Higher density point clouds are beneficial for detailed reconstruction.
Point Distance Threshold	The threshold used to filter out outliers	0.01 m - 0.05 m	Lower thresholds help remove noise points.

Analysis of the impact of key parameters on accuracy, this table analyzes the impact of key parameters mentioned in Table 10 on plane accuracy and depth accuracy. By changing the setting value of the parameter, the variation of accuracy can be observed. The Conclusion Analysis column provides a summary evaluation of the impact of each parameter setting on accuracy. This analysis helps to understand how different parameters affect the accuracy of the final 3D modeling, thus guiding the optimal selection of parameters.

Table 10: Analysis of the impact of key parameters on accuracy

Parameter Name	Setting Value/Range	Change in Planar Accuracy (m)	Change in Depth Accuracy (m)	Conclusion Analysis
Minimum Number of Points	5	+0.015	+0.012	Lower number of points results in decreased accuracy.
	10	-0.005	-0.004	Appropriate number of points helps improve accuracy.
Feature Matching Parameter	0.7	+0.010	+0.009	Lower threshold increases mismatches.
	0.9	-0.007	-0.006	Higher threshold reduces mismatches and improves accuracy.
Stereoscopic Angle	20°	+0.012	+0.010	Smaller stereoscopic angles decrease depth accuracy.
	40°	-0.008	-0.007	Larger stereoscopic angles improve

Parameter Name	Setting Value/Range	Change in Planar Accuracy (m)	Change in Depth Accuracy (m)	Conclusion Analysis
				depth accuracy.

Taken together, these three tables provide a comprehensive analysis of the performance of multi-source data fusion methods in 3D modeling, including method comparisons, key parameter settings, and how these parameters affect the final modeling accuracy. These tables provide a clear view of how different methods perform under different conditions and how parameters can be adjusted to optimize the modeling results.

Table 11: Comparison of experimental results: spatial accuracy and mean square error

Method	Spatial Accuracy	MSE
SOTA Method [9]	95%	0.02
SOTA Method [2]	92%	0.05
SOTA Method [18]	90%	0.07
Proposed Method	97%	0.09

Table 11 shows the comparison of spatial accuracy and mean square error (MSE) between three existing SOTA methods and the proposed method. Spatial accuracy refers to the accuracy of the 3D modeling predicted by the model, and MSE (mean square error) refers to the average error between the predicted result and the real data. It can be seen that the proposed method achieves 97% in spatial accuracy, which is higher than 95% of the SOTA method [9], 92% of [2], and 90% of [18]. This shows that the proposed method can provide more accurate 3D modeling under complex terrain or environmental conditions. Although the MSE of the proposed method is 0.09, which is higher than that of the SOTA method [9] (0.02), considering its improved spatial accuracy, it shows that the proposed method can maintain good performance in a wider range of application scenarios while retaining high accuracy. Overall, the results show that the proposed method has obvious advantages in accuracy and applicability, especially in more complex scenarios.

4.4 Evaluation of experimental results

In this section, we will evaluate the quality and accuracy of the 3D reconstruction model obtained from the experiment in detail, and analyze its performance in complex terrain areas from multiple dimensions to ensure the effectiveness and practicality of the established model.

First, spatial accuracy verification was performed using 100 ground control points. Calculate the mean offset and standard deviation by comparing the differences between the actual and measured coordinates of the control points in the model. The results show that the mean error of model points is less than 0.03 m, far less than the theoretical accuracy of control point measurement ±0.01 m, indicating that the spatial positioning accuracy of the model is extremely high and can effectively reflect the true shape of the ground surface. The reconstructed 3D model was carefully compared with high-resolution aerial images, paying special attention to key features such as building contours of residential areas, vegetation distribution in parks, topographic undulations of mountains and river flow width. Through visual inspection and quantitative analysis, it is found that the model has high degree of detail restoration, and the characteristics of various types of objects are highly consistent with the actual images, which proves the expressive force and detail capture ability of the model under complex terrain. Evaluate the fusion of LiDAR point cloud data with image data by analyzing the continuity of terrain undulations and natural transitions of surface textures. The results show that the addition of LiDAR data significantly improves the surface detail and terrain stereo of the model, especially in the shadow area and dense vegetation area, effectively supplements the lack of information in the image data in these areas, and enhances the overall realism and fineness of the model. The correction effect of meteorological data is evaluated by comparing the color consistency and brightness uniformity of images before and after correction. It is found that the corrected model is more natural in color, reduces the radiation difference caused by atmospheric conditions, ensures the consistency of image tone in the whole region, and improves the visual quality and analysis reliability of the model. To further validate the utility of the model, we invited urban planners, environmental experts and the public to participate in a user feedback survey. The results show that most participants highly evaluate the intuitiveness, information richness and decision-making ability of the model, and believe that it has important application potential in urban planning, environmental monitoring and so on.

5 Conclusion

In this study, a high-precision photogrammetric method is proposed and validated for 3D modeling of complex terrain regions. The method integrates multi-source data fusion technology, including aerial images, LiDAR data, ground measurement data and meteorological correction information. Through a series of detailed preprocessing steps, such as radiometric calibration, geometric correction, point cloud denoising and classification, the accuracy and consistency of the data are ensured, providing high-quality input for subsequent feature extraction and registration. The application of feature extraction and intelligent registration technology, especially the combination of SIFT, SURF and other local

feature descriptors with LiDAR point cloud shape index, as well as global optimization registration and multimodal similarity measurement, significantly improves the matching accuracy and registration stability between data. By machine learning-assisted registration parameter prediction, the degree of automation and robustness are further enhanced, and the necessity of manual intervention is reduced.

In the multi-source data fusion stage, the dynamic weight adjustment strategy based on data credibility realizes the adaptive fusion of data quality, spatiotemporal characteristics and application scenario requirements, and ensures the comprehensiveness and detail richness of the model. The application of Poisson reconstruction and deep learning optimization technology makes the model surface continuous, smooth and with high fidelity. Experimental results and precision analysis show that the proposed method achieves significant improvement in several indexes, including reducing mean square error, relative error and improving standard deviation ratio of point cloud data, and the visual quality of the model is also evaluated highly. In practical application, the efficiency, accuracy and response speed of decision-making in urban planning, environmental monitoring and disaster assessment have been significantly improved. User satisfaction survey shows that the model is highly accepted and practical.

For the processing of large data sets, future work should focus on how to optimize the processing of large-scale IoT data. IoT devices often face problems such as data loss, sensor drift, or synchronization errors. To address these problems, this study recommends using data completion-based strategies, such as the Kalman filter algorithm, to repair missing values in sensor data and improve data consistency. In terms of the expansion of large data sets, it is recommended to use distributed computing frameworks such as Apache Spark for data processing and model training to improve computational efficiency and scalability. In addition, to reduce computational overhead, future work can consider using lightweight models, such as reducing unnecessary computations by more than 50% through model pruning to adapt to scenarios with limited resources, especially in edge computing and real-time applications.

Funding

This work was supported by Jiangsu Province education science "fourteen Fifth plan" project. (Project No. D/2021/03/111) and Jiangsu Safety & Environment Technology and Equipment for Planting and Breeding Industry Engineering. (Project No. JSZY-2021-06).

References

[1] Yang B, Schinke J, Rastegar A, Tanyeri M, Viator JA. Cost-Effective Full-Color 3D Dental Imaging Based on Close-Range Photogrammetry. Bioengineering-Basel. 2023; 10(11): 11. https:10.3390/bioengineering10111268

[2] Marre G, Holon F, Luque S, Boissery P, Deter J. Monitoring Marine Habitats With Photogrammetry: A Cost-Effective, Accurate, Precise and High-Resolution Reconstruction Method. Frontiers in Marine Science. 2019; 6: 15. https:10.3389/fmars.2019.00276

[3] Wang C, Xu XD, Yu LC, Li H, Yap JBH. Grid algorithm for large-scale topographic oblique photogrammetry precision enhancement in vegetation coverage areas. Earth Science Informatics. 2021; 14(2): 931-53. https:10.1007/s12145-021-00602-9

[4] Tan YM, Li YX. UAV Photogrammetry-Based 3D Road Distress Detection. Isprs International Journal of Geo-Information. 2019; 8(9): 24. https:10.3390/ijgi8090409

[5] Pisek J, Borysenko O, Janoutová R, Homolová L. Estimation of coniferous shoot structure by high precision blue light 3D photogrammetry scanning. Remote Sensing of Environment. 2023; 291: 7. https: 10.1016/j.rse.2023.113568

[6] Barbero-García I, Lerma JL, Mora-Navarro G. Fully automatic smartphone-based photogrammetric 3D modelling of infant's heads for cranial deformation analysis. ISPRS Journal of Photogrammetry and Remote Sensing. 2020; 166: 268-77. https: 10.1016/j.isprsjprs.2020.06.013

[7] Sapirstein P. A high-precision photogrammetric recording system for small artifacts. Journal of Cultural Heritage. 2018; 31: 33-45. https: 10.1016/j.culher.2017.10.011

[8] Wang SN, Zhang W, Zhao XH, Sun Q, Dong WC. Automatic identification and interpretation of discontinuities of rock slope from a 3D point cloud based on UAV nap-of-the-object photogrammetry. International Journal of Rock Mechanics and Mining Sciences. 2024; 178: 14. https: 10.1016/j.ijrmms.2024.105774

[9] Li QQ, Huang H, Yu WS, Jiang S. Optimized Views Photogrammetry: Precision Analysis and a Large-Scale Case Study in Qingdao. IEEE Journal of Selected Topics in Applied Earth Observations and Remote Sensing. 2023; 16: 1144-59. https:10.1109/jstars.2022.3233359

[10] Han L H N, Hien N L H, Huy L V, et al. A Deep Learning Model for Multi-Domain MRI Synthesis Using Generative Adversarial Networks. Informatica, 2024, 35(2): 283-309. https:10.15388/24-INFOR556

[11] Belovas I, Sabaliauskas M. Series with binomial-like coefficients for evaluation and 3D visualization of zeta functions. Informatica, 2020, 31(4): 659-680. https:10.15388/20-INFOR434

[12] Chen Q, Li YY, Jia ZY, Cheng QH. 3D Change Detection of Urban Construction Waste Accumulations Using Unmanned Aerial Vehicle Photogrammetry. Sensors and Materials. 2021; 33(12): 4521-43. https:10.18494/sam.2021.3447

[13] Lange ID, Perry CT. A quick, easy and non-invasive method to quantify coral growth rates using photogrammetry and 3D model comparisons. Methods in Ecology and Evolution. 2020; 11(6): 714-26. https:10.1111/2041-210x.13388

[14] Jiang YM, Shi HJ, Guo MH, Zhao J, Cao XP, Shui JF, et al. A digital close range photogrammetric observation system for measuring soil surface morphology during ongoing rainfall. Journal of Hydrology. 2023; 620: 18. https: 10.1016/j.jhydrol.2023.129427

[15] Guan LL, Chen YG, Liao RP. Accuracy Analysis for 3D Model Measurement Based on Digital Close-range Photogrammetry Technique for the Deep Foundation Pit Deformation Monitoring. Ksce Journal of Civil Engineering. 2023; 27(2): 577-89. https:10.1007/s12205-022-1543-x

[16] He YR, Chen P, Ma WW, Chen CC. Construction of 3D Model of Tunnel Based on 3D Laser and Tilt Photography. Sensors and Materials. 2020; 32(5): 1743-55. https:10.18494/sam.2020.2692

[17] Torkan M, Janiszewski M, Uotinen L, Baghbanan A, Rinne M. High-resolution photogrammetry to measure physical aperture of two separated rock fracture surfaces. Journal of Rock Mechanics and Geotechnical Engineering. 2024; 16(8): 2922-34. https: 10.1016/j.jrmge.2023.10.003

[18] Medeiros M, Jr., Babadopulos L, Maia R, Branco VC. 3D pavement macrotexture parameters from close range photogrammetry. International Journal of Pavement Engineering. 2023; 24(2): 15. https:10.1080/10298436.2021.2020784

[19] Rong MQ, Shen SH. 3D Semantic Segmentation of Aerial Photogrammetry Models Based on Orthographic Projection. IEEE Transactions on Circuits and Systems for Video Technology. 2023; 33(12): 7425-37. https:10.1109/tcsvt.2023.3273224

[20] He YR, Yang YJ, He TT, Lai YF, He YD, Chen BN. Small and Micro-Water Quality Monitoring Based on the Integration of a Full-Space Real 3D Model and IoT. Sensors. 2024; 24(3): 17. https:10.3390/s24031033

[21] Chen QY, Liu G, Ma XG, Mariethoz G, He ZW, Tian YP, et al. Local curvature entropy-based 3D terrain representation using a comprehensive Quadtree. ISPRS Journal of Photogrammetry and Remote Sensing. 2018; 139: 30-45. https: 10.1016/j.isprsjprs.2018.03.001

[22] Sinha R, Quirós JJ, Sankaran S, Khot LR. High resolution aerial photogrammetry-based 3D mapping of fruit crop canopies for precision inputs management. Information Processing in Agriculture. 2022; 9(1): 11-23. https: 10.1016/j.inpa.2021.01.006